Journal Pre-proof

Engineered dynamic distribution of malonyl-CoA flux for improving polyketide biosynthesis in *Komagataella phaffii*

Jiao Wen<ce:contributor-role>Writing-original draft), Lin Tian, Qi Liu, Yuanxing Zhang<ce:contributor-role>Writing-review and editing), Menghao Cai<ce:contributor-role>Writing-review and editing)

PII: S0168-1656(20)30159-0

DOI: https://doi.org/10.1016/j.jbiotec.2020.06.012

Reference: BIOTEC 8671

To appear in: *Journal of Biotechnology*

Received Date: 17 April 2020

Revised Date: 27 May 2020

Accepted Date: 16 June 2020

Please cite this article as: Wen J, Tian L, Liu Q, Zhang Y, Cai M, Engineered dynamic distribution of malonyl-CoA flux for improving polyketide biosynthesis in *Komagataella phaffii*, *Journal of Biotechnology* (2020), doi: https://doi.org/10.1016/j.jbiotec.2020.06.012

Engineered dynamic distribution of malonyl-CoA flux for improving polyketide biosynthesis in *Komagataella phaffii*

Jiao Wen[a], Lin Tian[a], Qi Liu[a], Yuanxing Zhang[a,b], Menghao Cai[a,*]

[a] State Key Laboratory of Bioreactor Engineering, East China University of Science and Technology, 130 Meilong Road, Shanghai 200237, China

[b] Shanghai Collaborative Innovation Center for Biomanufacturing, 130 Meilong Road, Shanghai 200237, China

Corresponding Author (Menghao Cai)

* E-mail address: cmh022199@ecust.edu.cn. Tel.: +86-21-64253306.

Graphical abstract

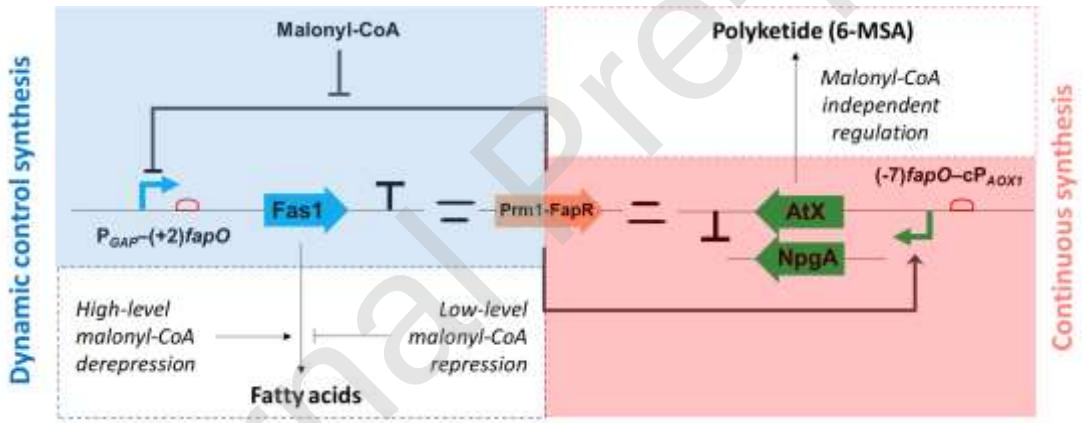

Highlights

- A synthetic malonyl-CoA independent module allowed continuous polyketide synthesis
- A synthetic malonyl-CoA dependent module dynamically regulated fatty acid synthesis
- An integrated biosystem redirected malonyl-CoA flux to improve polyketide synthesis

ABSTRACT

Malonyl-CoA is a basic but limited precursor for the biosynthesis of various bioactive compounds and life-supporting fatty acids in cells. This study develops a biosynthetic system to dynamically redirect malonyl-CoA flux and improve production of malonyl-CoA derived polyketide (6-MSA) in *Komagataella phaffii*. A synthetic regulatory protein fusing a yeast activator Prm1 with a bacterial repressor FapR was proved to work with a hybrid promoter (-7)*fapO*-cP$_{AOX1}$ and activate gene expression. Expression mode by the Prm1-FapR/(-7)*fapO*-cP$_{AOX1}$ device was not affected by intracellular malonyl-CoA levels. Further, 9 promoter variants of P$_{GAP}$ with insertion of *fapO* at various sites were tested with the Prm1-FapR. It generated a biosensor of Prm1-FapR/P$_{GAP}$-(+2)*fapO* with regulation behavior of malonyl-CoA-low-level repression/high-level derepression. Both devices were subsequently integrated into a single cell, for which fatty acid synthesis module was driven by Prm1-FapR/P$_{GAP}$-(+2)*fapO* but 6-MSA synthesis module was expressed by Prm1-FapR/(-7)*fapO*-cP$_{AOX1}$. The integrated system allowed continuous polyketide synthesis but malonyl-CoA-high-level "on"/low-level "off" fatty acid synthesis. This design finally increased 6-MSA production capacity by 260%, proving the positive effects of dynamic malonyl-CoA distribution to the target compounds. It provides a new strategy for synthesis of malonyl-CoA derived compounds in eukaryotic chassis hosts.

Keywords: *Komagataella phaffii*; FapR/*fapO*; Malonyl-CoA; Dynamic control; Synthetic biology

1. Introduction

With the development of synthetic biology, heterologous production of bioactive compounds in a chassis host has been commonly used (Galanie et al., 2015). However, precursor deficiency in cells often limits the final productivity of these compounds (Nielsen and Keasling, 2016). Malonyl coenzyme A (malonyl-CoA) is a basic building block for the biosynthesis of various value-added bioactive chemicals such as polyketide and flavonoid (Johnson et al., 2017). However, the flux of intracellular malonyl-CoA is strictly controlled because malonyl-CoA is also the precursor of fatty acids (FAs) and lipids, which are essential for life support (Li et al., 2015; Pitera et al., 2007). With a certain amount of malonyl-CoA, cells will preferentially produce FAs rather than other derivatives , leading to high difficulty in artificial regulation and affecting the synthesis of a series of downstream

compounds (Li et al., 2015; Pitera et al., 2007).

For metabolic regulation, dynamic control is an effective strategy that can increase the productivity of engineered strains and make them more robust to the changing conditions (Holtz and Keasling, 2010). It allows cells equipped with engineered sensing system regulating input/output flux dynamically (Holtz and Keasling, 2010). The synthetic cells would respond to variation of a key intermediate inside the cell and regulate the target and competitive pathways accordingly (Holtz and Keasling, 2010). To present, use of dynamic control to improve biosynthesis of value-added chemicals has achieved good progress in *Escherichia coli*. A typical work has been reported that a regulatory circuit sensing acetyl phosphate was designed and used to improve lycopene biosynthesis in *E. coli* (Farmer and Liao, 2000). An acyl-CoA responsive system (Zhang et al., 2012) and an oscillatory malonyl-CoA metabolism (Xu et al., 2014) were reported to increase the production of FAs or their derivatives in *E. coli*. But till now, design of dynamic metabolic control in yeast or higher eukaryotic microorganisms is still quite limited (David et al., 2016; Li et al., 2015).

The methylotrophic yeast, *Komagataella phaffii* (syn *Pichia pastoris*), is often used as an excellent chassis cell to produce heterologous proteins due to its easy-culture, high-density growth, intensive expression capacity and post-translational modification (Schwarzhans et al., 2017; Peña et al., 2018; Yang and Zhang, 2018). Recently, it is also recognized as good chassis host for production of small molecule pharmaceuticals such as polyketides (Schwarzhans et al., 2017; Peña et al., 2018; Yang and Zhang, 2018). In cells, inadequate malonyl-CoA usually limits the production capacity of its derived bioactive compounds (David et al., 2016; Johnson et al., 2017). Thus, engineering of malonyl-CoA metabolism has been widely concerned to improve the product titer (David et al., 2016; Johnson et al., 2017). It was reported that the bacterial regulatory protein FapR could bind with malonyl-CoA, which then hampered the binding of FapR with its operator *fapO* and regulated gene transcription (Schujman et al., 2003; 2006). In our previous work, we constructed a synthetic malonyl-CoA metabolic oscillator that recurrently regulates malonyl-CoA source pathway and sink pathway for 6-methylsalicylic acid (6-MSA, a model fungal polyketide) synthesis in *K. phaffii* (Wen et al., 2020). Nevertheless, the resulted "on" and "off" states of gene expression caused less accumulation of 6-MSA synthase (AtX) than the constitutive expression,

leading to a low 6-MSA level (Wen et al., 2020). As polyketide and FAs competitively use malonyl-CoA as a key precursor, regulation of FAs synthesis might benefit production of polyketide. The synthesis of cytosolic FAs in yeast is mainly carried out by the fatty acid synthase (Fas) with Fas1 and Fas2 subunits (Inokoshi et al., 1994; Tehlivets et al., 2007). Fas1 and Fas2 are often present in equimolar amounts in Fas complex, however, the activity of Fas holoenzyme is mainly determined by the amount of Fas1 (Inokoshi et al., 1994; Tehlivets et al., 2007). Therefore, regulation of Fas1 expression might achieve the purpose of regulating FAs biosynthetic pathway.

In this study, we proposed an improved strategy that involves a malonyl-CoA independent expression of AtX and malonyl-CoA dependent expression of Fas (Fas1). Accordingly, 6-MSA biosynthetic pathway will always keep "on", but its competitive pathway for FAs synthesis will only be "on" with high-level malonyl-CoA but "off" with low-level malonyl-CoA. By this design, the engineered cells will preferentially use malonyl-CoA for 6-MSA synthesis. The developed gene circuits are useful for potential biosynthetic applications of malonyl-CoA derived compounds not limited by natural cellular behavior.

2. Materials and methods

2.1. Materials and molecular agents

The plasmid pPGG (Amp^R expression cassette removed from the pPIC3.5K) was constructed previously (Wang et al., 2016). Other materials and molecular agents are the same as our previous study (Wen et al., 2020).

2.2. Construction of plasmids and strains

For expression of the fused regulator Prm1-FapR, a fragment *Prm1-FapR* cloned from pAG_Prm1-FapR (Wen et al., 2020) by primer pair of IPFF/IPFR was fused with the P_{ICL1} promoter (cloned by primer pair of IF/IR from *K. phaffii* genome), generated a plasmid of pAG_P_{ICL1}-Prm1-FapR. Then this plasmid was linearized by primer pair of ICL1-linear-F/ICL1-linear-R and transformed into *K. phaffii* GS115, resulting in the strain named GS_IPF. This strain was used as a parent strain for further construction. The plasmid of pGZB_P_{GAP}-(+2)*fapO*-eGFP (Wen et al., 2020) was linearized by *BspQ*I and transformed into the GS_IPF strain, giving a strain of GS_IPF_P_{GAP}-(+2)*fapO*-eGFP. For strains with *fapO* inserted at various locations, their construction procedure

referred to the GS_IPF_P_{GAP}-(+2)*fapO*-eGFP. Similarly, the pGZB_(-7)*fapO*-cP_{AOX1}-eGFP plasmid (Wen et al., 2020) was linearized by *BspQ*I and transformed into the GS_IPF strain, giving a strain of GS_IPF_(-7)*fapO*-cP_{AOX1}-eGFP. The linearized pGZB_P_{GAP}-(+2)*fapO*-eGFP and pGZB_(-7)*fapO*-cP_{AOX1}-eGFP plasmids were integrated into *K. phaffii* GS115 genome at the *GAP* site. We added *GAP* additionally, as there is no *GAP* homologous sequence in the pGZB_(-7)*fapO*-cP_{AOX1}-eGFP plasmid (Wen et al., 2020). All transformations were identified and confirmed by PCR and gene sequencing. Strains carrying single copy of each specific cassette were selected for analysis.

To construct the biosynthetic pathway of a model fungal polyketide 6-methylsalicylic acid (6-MSA) (Wattanachaisaereekul et al., 2007), *atX* and *npgA* gene fragments were firstly obtained from the strain of GS_XN (Xu et al., 2019) by primer pairs of atXF2/atXR2 and npgAF2/ngpAR2, respectively. A plasmid backbone was then cloned from the pGZB_(-7)*fapO*-cP_{AOX1}-eGFP by primer pair of fcaF/fcaR or fcnF/fcnR, which was then fused with the obtained *atX* or *npgA* and generated the plasmid of pGZB_(-7)*fapO*-cP_{AOX1}-*atX* or pGZB_(-7)*fapO*-cP_{AOX1}-*ngpA*, respectively. Then the (-7)*fapO*-cP_{AOX1}-*atX* cassette was cloned by primer pair of atXcasF3/atXcasR3, and fused into the *Spe*I linearized pPICZ B, resulting in a plasmid of pZB_(-7)*fapO*-cP_{AOX1}-*atX*. It was linearized by *Spe*I again and fused with (-7)*fapO*-cP_{AOX1}-*ngpA* cloned from the pGZB_(-7)*fapO*-cP_{AOX1}-*ngpA* by primer pair of atXcasF3/atXcasR3, which generated a plasmid of pZB_(-7)*fapO*-cP_{AOX1}-*atX*+*ngpA* finally. The plasmid was linearized by *Pme*I and integrated into the genome of *K. phaffii* GS115 and GS_IPF at *AOX1* site to give strains of GS_(-7)*fapO*-cP_{AOX1}-AtX+NpgA and GS_IPF_(-7)*fapO*-cP_{AOX1}-AtX+NpgA, respectively. For construction of pZB_P_{ICL1}-*atX*-*ngpA*, a fragment of P_{ICL1} was firstly obtained from *K. phaffii* genome by primer pair of IF3/IR3 or IF4/IR4, respectively. Plasmid backbone was then cloned from the pGZB_P_{GAP}-*atX* or pGZB_P_{GAP}-*ngpA* by primer pair of IaF/IaR or InF/InR, which was then fused with the obtained P_{ICL1} fragments, generating the plasmid of pGZB_P_{ICL1}-*atX* or pGZB_P_{ICL1}-*ngpA*, respectively. Then the P_{ICL1}-*atX* cassette was cloned by primer pair of atXcasF2/atXcasR2, and fused into the *Spe*I linearized pPICZ B, resulting in a plasmid of pZB_P_{ICL1}-*atX*. It was linearized by *Spe*I again and fused with P_{ICL1}-*ngpA* cloned from pGZB_P_{ICL1}-*ngpA* by primer pair of atXcasF2/atXcasR2, which generated pZB_P_{ICL1}-*atX*+*ngpA* finally. It was then linearized by *Pme*I and integrated into the *K. phaffii* GS115 genome at *AOX1* site to give the GS_P_{ICL1}-AtX+NpgA strain. To construct the *fas1* pathway, *fas1**

(the upstream 1200 bp of the native *fas1*, GenBank accession no. **NC012963**) was cloned from *K. phaffii* genome by primer pair of fas1upF/fas1upR and fused into pPGG backbone cloned by primer pair of GfF/GfR, producing a plasmid of p3.5K*_P_{GAP}-*fas1**. For construction of p3.5K*_P_{GAP}-(+2)*fapO-fas1**, the P_{GAP}-(+2)*fapO* fragment was firstly obtained from the pGZB_P_{GAP}-(+2)*fapO*-eGFP plasmid by primer pair of 2GF/2GR, which was fused into the p3.5K*_P_{GAP}-*fas1** backbone by primer pair of GffF/GffR by seamless cloning, producing a plasmid of p3.5K*_P_{GAP}-(+2)*fapO-fas1**. Then they were linearized by primer pair of fas1-linear-F/fas1-linear-R and transformed into the GS_IPF_(-7)*fapO*-cP_{AOX1}-AtX+NpgA strain, resulting in the final strain of GS_IPF_(-7)*fapO*-cP_{AOX1}-AtX+NpgA_P_{GAP}-Fas1 (control) and GS_IPF_(-7)*fapO*-cP_{AOX1}-AtX+NpgA_P_{GAP}-(+2)*fapO*-Fas1 (dynamic). The native *fas1* gene in both strains were destroyed and allowed an intact *fas1* driven by P_{GAP} or P_{GAP}-(+2)*fapO* solely. All the primers were listed in Appendix A. Table S1. Information of all the constructed strains was shown in Appendix A. Table S2. The hybrid promoters with *fapO* inserted at different sites were listed in Appendix A. Table S3.

2.3. Evaluation of the engineered biological devices and quantification of 6-MSA

For evaluation of the engineered biological devices, 12 mg/L cerulenin was added to the broth to force cells to accumulate malonyl-CoA after the constructed strains were grown at 30°C and 200 *rpm* for about 12 h in YNE (1.34% YNB+1% ethanol) medium (Wen et al., 2020). The fluorescence intensity of eGFP was used to characterize the activity of the engineered biological devices, which was performed following the procedures we reported (Wen et al., 2020). For 6-MSA quantification, strains were grown (200 *rpm*, 30°C) in YNE medium after seed preparation, 6-MSA was extracted every 24 h till 96 h. The extraction and quantification of 6-MSA were performed following the procedures we reported (Wen et al., 2020). All experiments were performed in triplicates.

2.4. Statistical analysis

The data were obtained from three biological replicates assayed in duplicate or triplicate. The independent-sample t-test was used to analyze the differences among grouped data. Statistical significance was assessed at $P<0.05$.

3. Results and discussion

3.1. Construction of 6-MSA synthase expression module independent of malonyl-CoA regulation

We previously developed a series of transcriptional signal activation devices named Prm1-FapR/*fapO*-cP$_{AOX1}$, for which 18 hybrid promoter variants that carrying the operator sequence (*fapO*) of FapR were constructed. The Prm1-FapR fusion protein then converted the bacterial transcriptional repressor FapR to a yeast transcriptional activator (Fig. 1A). For this, Prm1-FapR binds to *fapO*, recruiting RNA polymerase for the hybrid promoter of *fapO*-cP$_{AOX1}$ (Wen et al., 2020).

For *K. phaffii*, its cytosolic malonyl-CoA easily reached a high level when culturing on ethanol (Liu et al., 2019). Thus, it is beneficial for polyketide production using ethanol as substrate in this yeast (Liu et al., 2019). As the expression of transcription factor will influence the intensity of activation (D'Ambrosio and Jensen, 2017), we then used an ethanol-inducible promoter P$_{ICL1}$ (Menendez et al., 2003) to drive Prm1-FapR expression. The intensity of P$_{ICL1}$ reached about 7 times as that of the P$_{PRM1}$ (Wen et al., 2020) when using eGFP as a reporter (Appendix A. Fig. S1). The resulted transcriptional signal activation device P$_{ICL1}$_Prm1-FapR/(-7)*fapO*-cP$_{AOX1}$ achieved strong activation effect and led to high levels of eGFP (Fig. 1B). Different from the malonyl-CoA dependent device of P$_{PRM1}$_Prm1-FapR/(-52)*fapO*-cP$_{AOX1}$ (Wen et al., 2020), the eGFP expression by the P$_{ICL1}$_Prm1-FapR/(-7)*fapO*-cP$_{AOX1}$ with *fapO* located 6 bp upstream of cP$_{AOX1}$ (Appendix A. Table S3) was almost not affected by cerulenin (12 mg/L). As is known, cerulenin can block FAs/polyketide biosynthetic pathway and force cells to accumulate malonyl-CoA (Schujman et al., 2006; 2008). The unchanged eGFP expression implied that the device was not affected by variation of intracellular malonyl-CoA level (Fig. 1C). Also, the expression of eGFP by the P$_{ICL1}$_Prm1-FapR/(-7)*fapO*-cP$_{AOX1}$ reached about two folds of that by the P$_{ICL1}$ (Fig. 1B). The transcriptional signal amplification effect was further verified by 6-MSA biosynthesis. The 6-MSA synthase (AtX) and phosphopantetheinyl transferase (NpgA) were expressed by the P$_{ICL1}$_Prm1-FapR/(-7)*fapO*-cP$_{AOX1}$, resulting 6-MSA production of about two folds as that by the P$_{ICL1}$ (Fig. 1D).

3.2. Construction of FAs synthase expression module dynamically regulated by malonyl-CoA

Malonyl-CoA acts as a key precursor for biosynthesis of both FAs and polyketide. However, the inadequate malonyl-CoA in cells usually limits the production capacity of malonyl-CoA derived chemicals (David et al., 2016; Johnson et al., 2017). Therefore, it is necessary to regulate FAs

synthesis, which allows cells preferentially use malonyl-CoA for synthesis of polyketide but not FAs. However, as FAs play critical roles in life support (Li et al., 2015; Pitera et al., 2007), it is not sensible to knock out the FAs synthetic pathway absolutely. We then conceive a strategy that repressing FAs synthesis under low malonyl-CoA level and activating it when malonyl-CoA is sufficient. In theory the cells will synthesize polyketide continuously but only allow FAs synthesis when malonyl-CoA is adequate.

In our previous work, we constructed a series of malonyl-CoA sensors named Prm1-FapR/P_{GAP}-*fapO*, for which 24 promoter variants of the P_{GAP} promoter with insertion of *fapO* inside were designed (Wen et al., 2020). Therein, the Prm1-FapR binds to *fapO* and highly repressed the promoter activity at low malonyl-CoA level when *fapO* inserted at -2~+27 site relative to the P_{GAP} TATA-box. The derepression behavior then happened with increased malonyl-CoA level by cerulenin (Wen et al., 2020). Therefore, these sensors could be used for our dynamic control of FAs synthesis in this work. While expression of Prm1-FapR was driven by the P_{ICL1} but not the previous P_{PRM1} in this work, we then integrated the P_{ICL1}_Prm1-FapR and P_{GAP}-*fapO* with *fapO* at -2~+27, respectively (Fig. 2A). The eGFP fluorescence intensity of each construct was shown in Fig. 2B. As discussed above, synthesis of FAs should not be absolutely blocked. On the other hand, FAs synthesis is competitive to the production of target compound, thus its biosynthetic pathway should not be strong. Thus, the P_{ICL1}_Prm1-FapR/P_{GAP}-(+2)*fapO* with the lowest eGFP fluorescence intensity was selected as the potential sensor for the control of FAs biosynthesis. We further verified the malonyl-CoA dependent repression/de-repression regulation mode of this biosensor. The eGFP expression by the P_{ICL1}_Prm1-FapR/P_{GAP}-(+2)*fapO* was repressed by 65% compared with that by the P_{GAP}-(+2)*fapO* solely (Fig. 2C). However, when 12 mg/L cerulenin was added, a remarkable derepression effect was observed. The increased malonyl-CoA level by cerulenin released eGFP expression by 110% (Fig. 2C). Therefore, this malonyl-CoA dependent repression/de-repression sensor can be applied for the dynamic control of FAs biosynthesis.

3.3. Integration of the malonyl-CoA independent 6-MSA synthase expression module and dependent FAs synthase expression module

Theoretically, with the above synthetic gene circuits the malonyl-CoA flux will be redirected from synthesis of FAs toward 6-MSA, while the FAs pathway will be finetuned by varying malonyl-

CoA. It should lead to a more efficient biosynthetic system for 6-MSA. To verify it, we then integrate two synthetic devices into a single cell. For this, the malonyl-CoA sink pathway (6-MSA synthase and phosphopantetheinyl transferase encoded by *atX* and *npgA* respectively) was placed under the control of the P_{ICL1}_Prm1-FapR/(-7)*fapO*-cP_{AOX1}; A cassette of P_{GAP}-(+2)*fapO-fas1** was inserted into the upstream of genomic *fas1*, which destroyed the endogenous *fas1* and allowed an intact *fas1* controlled by the P_{ICL1}_Prm1-FapR/P_{GAP}-(+2)*fapO* for FAs synthesis (Fig. 3A).

Accordingly, the malonyl-CoA independent device was employed to drive 6-MSA production and the malonyl-CoA sensor was used for the dynamic control of FAs synthesis. When the substrate in medium is sufficient, the increased malonyl-CoA will promote binding of malonyl-CoA to Prm1-FapR and in turn facilitate dissociation of Prm1-FapR from P_{GAP}-(+2)*fapO*. It will switch on *fas1* expression and improve FAs synthesis for cell support. On the other hand, when the substrate in medium is inadequate, the limited malonyl-CoA will enable binding of Prm1-FapR to P_{GAP}-(+2)*fapO*. It will switch off *fas1* expression and FAs synthesis, which leaves more malonyl-CoA for 6-MSA synthesis. We compared two strains with *fas1* expression driven by the native P_{GAP} (control) without *fapO* and the malonyl-CoA sensor with P_{GAP}-(+2)*fapO* (dynamic). The engineered strain achieved a 6-MSA production of 9.8 mg/g dry cell weight (DCW) at 96 h, which was 2.6-fold higher than that of the control strain (Fig. 3B). Also, cell growth during the culture showed no significant differences (Appendix A. Fig. S2), indicating the engineered regulation of FAs synthesis could be fine for life support of yeast cells.

Till now, malonyl-CoA biosensor and its based dynamic control are seldom reported in yeast and other eukaryotes. In a previous work, David et al. (2016) operated intracellular malonyl-CoA level by glucose control, by which the varying malonyl-CoA directly switch on/off biosynthetic pathway of its derived product of 3-hydroxypropionic acid. This study proposed a different strategy that cells automatically sensing malonyl-CoA levels in order to switch on/off the competitive pathway of the malonyl-CoA derived target compound. By this strategy, cells can not only produce FAs for life support but also avoid excessive FAs generation, which redirects malonyl-CoA flux to promote 6-MSA synthesis. The developed biosynthetic system could also be used for dynamic distribution of malonyl-CoA flux for regulation of other malonyl-CoA derived chemicals. Besides, as a non-conventional yeast, *K. phaffii* has been widely used in protein expression for both academic

and industrial purpose. This strain holds various merits such as high cell density, easy culture, strong expression capacity, stable inheritance and mild glycosylation, which allows it an excellent host for protein expression (Gasser et al., 2013). These advantages also make it a potential chassis host for synthetic biology. Moreover, its good methanol-utilizing ability endows it a promising chassis host for biotransformation of methanol and other one-carbon substrates (Liu et al., 2018). However, the lack of tools for genetic operation and expression control severely limit its use in this area (Wagner and Alper, 2016). This work provides useful biological elements and devices that can be applied for fine-tuning expression control of synthetic pathways in *K. phaffii*.

4. Conclusion

This study reports an engineered dynamically controlled yeast biosynthetic system for improving biosynthesis of malonyl-CoA derived bioactive chemicals. This system allows continuous polyketide synthesis but automatically controlled competitive and essential FAs synthesis. The improved polyketide production proved the optimal distribution of malonyl-CoA flux to the target compounds. It provides an applicable method for efficient synthesis of malonyl-CoA derived compounds in eukaryotic chassis hosts.

Credit author statement

Jiao Wen: Performing experiments, Writing-Original draft preparation. **Lin Tian:** Performing experiments. **Qi Liu:** Designing. **Yuanxing Zhang:** Writing-Reviewing and Editing. **Menghao Cai:** Conceiving and Designing, Writing-Reviewing and Editing.

Declaration of interests

The authors declare that they have no known competing financial interests or personal relationships that could have appeared to influence the work reported in this paper.

Acknowledgements

This work was supported by the Fundamental Research Funds for the Shanghai Science and Technology Innovation Action Plan (17JC1402400), National Natural Science Foundation of China (31870073), Shanghai Rising-Star Program, China (19QA1402700), the 111 Project of China (B18022), Fundamental Research Funds for the Central Universities, China (22221818014) and Research Program of State Key Laboratory of Bioreactor Engineering.

References

D'Ambrosio, V., Jensen, M.K., 2017. Lighting up yeast cell factories by transcription factor-based biosensors. FEMS Yeast Res. 17, fox076. https://doi.org/10.1093/femsyr/fox076.

David, F., Nielsen, J., Siewers, V., 2016. Flux control at the malonyl-CoA node through hierarchical dynamic pathway regulation in *Saccharomyces cerevisiae*. ACS Syn. Biol. 5, 224–233. https://doi.org/10.1021/acssynbio.5b00161.

Farmer, W.R., Liao, J.C., 2000. Improving lycopene production in *Escherichia coli* by engineering metabolic control. Nat. Biotechnol. 18, 533–537. https://doi.org/10.1038/75398.

Galanie, S., Thodey, K., Trenchard, I.J., Filsinger, I.M., Smolke, C.D., 2015. Complete biosynthesis of opioids in yeast. Science 349, 1095–1100. https://doi.org/10.1126/science.aac9373.

Gasser, B., Prielhofer, R., Marx, H., Maurer, M., Nocon, J., Steiger, M., Puxbaum, V., Sauer, M., Mattanovich, D., 2013. *Pichia pastoris*: protein production host and model organism for biomedical research. Future Microbiol. 8, 191-208. https://doi.org/10.2217/fmb.12.133.

Holtz, W.J., Keasling, J.D., 2010. Engineering static and dynamic control of synthetic pathways. Cell 140, 0–23. https://doi.org/10.1016/j.cell.2009.12.029.

Inokoshi, J., Tomoda, H., Hashimoto, H., Watanabe, A., Takeshima, H., Omura, S., 1994. Cerulenin-resistant mutants of *Saccharomyces cerevisiae* with an altered fatty acid synthase gene. Mol. Gen. Genet. 244, 90−96. https://doi.org/10.1007/BF00280191.

Johnson, A.O., Gonzalez-Villanueva, M., Wong, L., Steinbüchel, A., Tee, K.L., Xu, P., Wong, T.S., 2017. Design and application of genetically-encoded malonyl-CoA biosensors for metabolic engineering of microbial cell factories. Metab. Eng. 44, 253–264. https://doi.org/10.1016/j.ymben.2017.10.011.

Li, S., Si, T., Wang, M., Zhao, H., 2015. Development of a synthetic malonyl-CoA sensor in

Saccharomyces cerevisiae for intracellular metabolite monitoring and genetic screening. ACS Syn. Biol. 4, 1308–1315. https://doi.org/10.1021/acssynbio.5b00069.

Liu, Y., Bai, C., Liu, Q., Xu, Q., Qian, Z., Peng, Q., Yu, J., Xu, M., Zhou, X., Zhang, Y., Cai, M., 2019. Engineered ethanol-driven biosynthetic system for improving production of acetyl-CoA derived drugs in Crabtree-negative yeast. Metab. Eng. 54, 275–284. https://doi.org/10.1016/j.ymben.2019.05.001.

Liu, Y., Tu, X., Xu, Q., Bai, C., Kong, C., Liu, Q., Yu, J., Peng, Q., Zhou, X., Zhang, Y., Cai, M., 2018. Engineered monoculture and co-culture of methylotrophic yeast for de novo production of monacolin J and lovastatin from methanol. Metab. Eng. 45, 189–199. https://doi.org/10.1016/j.ymben.2017.12.009.

Menendez, J., Valdes, I., Cabrera, N., 2003. The *ICL1* gene of *Pichia pastoris*, transcriptional regulation and use of its promoter. Yeast 20, 1097–1108. https://doi.org/10.1002/yea.1028.

Nielsen, J., Keasling, J.D., 2016. Engineering cellular metabolism. Cell 164, 1185–1197. https://doi.org/10.1016/j.cell.2016.02.004.

Peña, D.A., Gasser, B., Zanghellini, J., Steiger, M.G., Mattanovich, D., 2018. Metabolic engineering of *Pichia pastoris*. Metab. Eng. 50, 2–15. https://doi.org/10.1016/j.ymben. 2018.04.017.

Pitera, D.J., Paddon, C.J., Newman, J.D., Keasling, J.D., 2007. Balancing a heterologous mevalonate pathway for improved isoprenoid production in *Escherichia coli*. Metab. Eng. 9, 193–207. https://doi.org/10.1016/j.ymben.2006.11.002

Schujman, G.E., Altabe, S., Mendoza, D.D., 2008. A malonyl-CoA-dependent switch in the bacterial response to a dysfunction of lipid metabolism. Mol. Microbiol. 68, 987–996. https://doi.org/10.1111/j.1365-2958.2008.06202.x.

Schujman, G.E., Guerin, M., Buschiazzo, A., Schaeffer, F., Llarrull, L.I., Reh, G., Vila, A.J., Alzari, P.M., de Mendoza, D., 2006. Structural basis of lipid biosynthesis regulation in Grampositive bacteria. EMBO J. 25, 4074−4083. https://doi.org/10.1038/sj.emboj.7601284.

Schujman, G.E., Paoletti, L., Grossman, A.D., de Mendoza, D., 2003. FapR, a bacterial transcription factor involved in global regulation of membrane lipid biosynthesis. Dev. Cell 4, 663−672. https://doi.org/10.1016/S1534-5807(03)00123-0.

Schwarzhans, J.P., Luttermann, T., Geier, M., Kalinowski, J., Friehs, K., 2017. Towards systems

metabolic engineering in *Pichia pastoris*. Biotechnol. Adv. 35, 681–710. https://doi.org/10.1016/j.biotechadv.2017.07.009.

Tehlivets, O., Scheuringer, K., Kohlwein, S.D., 2007. Fatty acid synthesis and elongation in yeast. BBA-Mol. Cell Biol. L. 1771, 255−270. https://doi.org/10.1016/j.bbalip.2006.07.004.

Wagner JM, Alper HS., 2016. Synthetic biology and molecular genetics in non-conventional yeasts: Current tools and future advances. Fungal Genet. Biol. 89, 126–136. https://doi.org/10.1016/j.fgb.2015.12.001.

Wang, X., Wang, Q., Wang, J., Bai, P., Shi, L., Shen, W., Zhou, M., Zhou, X., Zhang, Y., Cai, M., 2016. Mit1 Transcription factor mediates methanol signaling and regulates the *alcohol oxidase 1* (*AOX1*) promoter in *Pichia pastoris*. J. Biol. Chem. 291, 6245−6261. http://doi.org/10.1074/jbc.M115.692053.

Wattanachaisaereekul, S., Lantz, A.E., Nielsen, M.L., Andrésson, O.S., Nielsen, J., 2007. Optimization of heterologous production of the polyketide 6-MSA in *Saccharomyces cerevisiae*. Biotechnol. Bioeng. 97, 893–900. https://doi.org/10.1002/bit.21286.

Wen, J., Tian, L., Xu, M., Zhou, X., Zhang, Y., Cai, M., 2020. A synthetic malonyl-CoA metabolic oscillator in *Komagataella phaffii*. ACS Syn. Biol. (in press) http://doi.org/10.1021/acssynbio.9b00378.

Xu, P., Li, L., Zhang, F., Zhang, F., Stephanopoulos, G., Koffas, M.A., 2014. Improving fatty acids production by engineering dynamic pathway regulation and metabolic control. Proc. Natl. Acad. Sci. USA. 111, 11299−11304. https://doi.org/10.1073/pnas.1406401111.

Xu, Q., Bai, C., Liu, Y., Song, L., Tian, L., Yan, Y., Zhou, J., Zhou, X., Zhang, Y., Cai, M., 2019. Modulation of acetate utilization in *Komagataella phaffii* by metabolic engineering of tolerance and metabolism. Biotechnol. Biofuels 12, 61. https://doi.org/10.1186/s13068-019-1404-0.

Yang, Z., Zhang, Z., 2018. Engineering strategies for enhanced production of protein and bio-products in *Pichia pastoris*: A review. Biotechnol. Adv. 3, 182–195. https://doi.org/10.1016/j.biotechadv.2017.11.002.

Zhang, F., Carothers, J.M., Keasling, J.D., 2012. Design of a dynamic sensor-regulator system for production of chemicals and fuels derived from fatty acids. Nat. Biotechnol. 30, 354−359.

https://doi.org/10.1038/nbt.2149.

Fig. 1. Construction and analysis of the malonyl-CoA independent biological device of P_{ICL1}_Prm1-FapR/(-7)*fapO*-cP_{AOX1}. (A) Construction scheme of the device. The grey arrow represents activation. (B) Expression of eGFP by (-7)*fapO*-cP_{AOX1}, P_{ICL1}, and P_{ICL1}_Prm1-FapR/(-7)*fapO*-cP_{AOX1}, respectively. n.s., statistically not significance. (C) Expression of eGFP was not affected by increased malonyl-CoA level by cerulenin (12 mg/L). (D) Production of 6-MSA by (-7)*fapO*-cP_{AOX1}, P_{ICL1} and P_{ICL1}_Prm1-FapR/(-7)*fapO*-cP_{AOX1}, respectively. (-7)A represents (-7)*fapO*-cP_{AOX1}; (-7)A+PF represents P_{ICL1}_Prm1-FapR/(-7)*fapO*-cP_{AOX1}. The fused transcription regulator Prm1-FapR was expressed by the promoter of P_{ICL1}. The hybrid promoter with *fapO* was shown in Appendix A. Table S3. All the error bars represent the standard deviation of three biological replicates assayed in triplicate. Statistical significance of the eGFP fluorescence intensity or 6-MSA production by the (-7)A+PF to that by the (-7)A or P_{ICL1} is at **P*<0.05 at each time point.

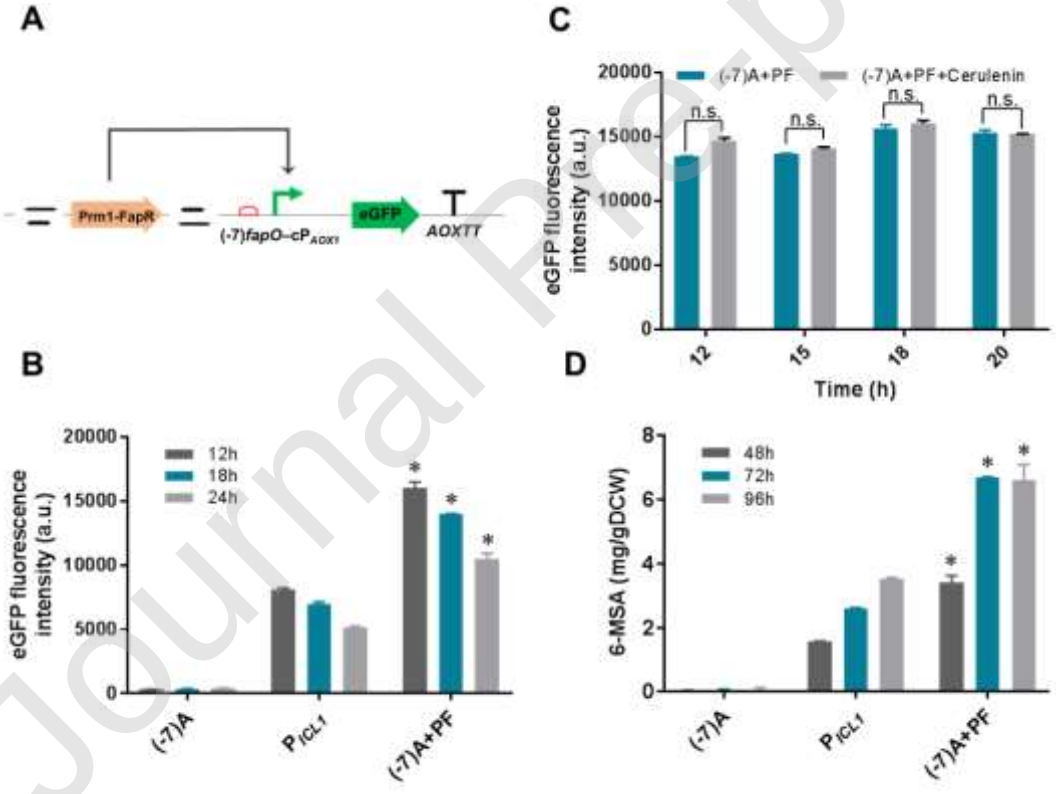

Fig. 2. Construction and analysis of the malonyl-CoA dependent biosensor of P_{ICL1}_Prm1-FapR/P_{GAP}-(+2)*fapO*. (A) Construction scheme of the sensor. The T lines means repression. (B) The eGFP fluorescence intensity expressed by various biological devices with *fapO* inserted at different

sites in P_{GAP}. (+2)G means P_{GAP}-(+2)*fapO*; PF means the Prm1-FapR expressed by the promoter of P_{ICL1}. The number indicates different *fapO* locations relative to the TATA box of P_{GAP} (refer to Appendix A. Table S3). Statistical significance of the eGFP fluorescence intensity by the (+2)G+PF to the other devices is at **P*<0.05 at each time point. (C) Repression/derepression regulation mode of the biosensor. The hybrid promoter of (+2)G was repressed the PF, while it was further derepressed by the increased malonyl-CoA level by cerulenin (12 mg/L). Statistical significance of the eGFP fluorescence intensity by the (+2)G+PF to (+2)G or (+2)G+cerulenin is at **P*<0.05 at 18 h. All the error bars represent the standard deviation of three biological replicates assayed in triplicate.

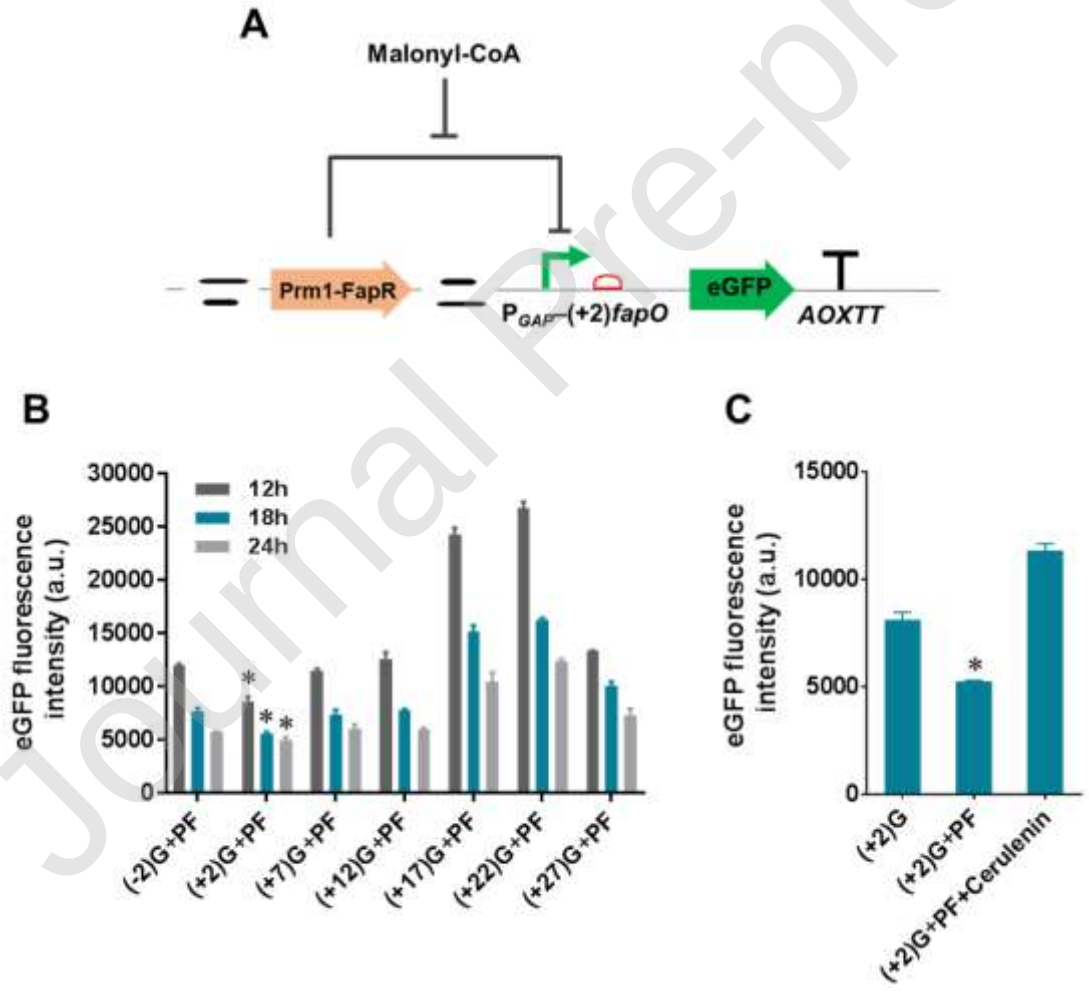

Fig. 3. Production of 6-MSA by the strain with integration of the malonyl-CoA independent 6-MSA

synthesis module and dependent fatty acid synthesis module. (A) Construction scheme of the dynamic control strain. Specific function of each device referred to Fig. 1A and Fig. 2A. The malonyl-CoA dependent biosensor in Fig. 2A was used to control fatty acid synthesis; the malonyl-CoA independent biological device in Fig. 1A was used to control 6-MSA synthesis. (B) Comparison of 6-MSA production by the control strain [(-7)A+PF+AtX+NpgA/G+PF+Fas] and dynamic strain [(-7)A+PF+AtX+NpgA/(+2)G+PF+Fas]. Strain construction and designation referred to Fig. 1 and Fig. 2. Statistical significance of 6-MSA production by the dynamic strain to the control strain is at $*P<0.05$ at each time point. All the error bars represent the standard deviation of three biological replicates assayed in triplicate. Fas1, fatty acid synthase; AtX, 6-MSA synthase; NpgA, phosphopantetheinyl transferase.